Effect of electromagnetic field on the slag resistance of MgO-C refractories

2011 IOP Conf. Ser.: Mater. Sci. Eng. 18 222003

(http://iopscience.iop.org/1757-899X/18/22/222003)

IOP Conf. Series: Materials Science and Engineering **18** (2011) 222003 doi:10.1088/1757-899X/18/22/222003

Effect of electromagnetic field on the slag resistance of MgO-C refractories

X C Li[1], **T X Wang, B Q Zhu**
The State Key Laboratory Cultivation Base of Refractories and Ceramics, Wuhan University of Science and Technology, Wuhan 430081, China

E-mail: lixiangcheng@wust.edu.cn

Abstract. The recent years have witnessed an unprecedented growth in the development and deployment of electromagnetic field(EMF) used in steel metallurgy. This paper investigates the effect of EMF on the slag resistance of MgO-C refractories. Using MgO-C refractories containing 14% carbon and the slag with a basicity(CaO/SiO_2) of around 0.8, the experiments of melting slag resistance of MgO-C refractories were carried out in an induction furnace and a resistance furnace. The results show that in induction furnace having EMF, the refractory sample corroded by the slag has an apparent penetration layer. $MgFe_2O_4$ phase is formed at a low temperature by MgO dissolved in Fe_2O_3. The low melting phases are monticellite ($CaMgSiO_4$, CMS) and forsterite (Mg_2SiO_4, MS). Under the condition of resistance furnace without EMF, scaling MgO dissolves into slag and reacts with Al_2O_3 to generate $MgAl_2O_4$ phase. The low melting phases are gehlenite ($Ca_2Al_2SiO_7$, C_2A_2S) and akermanite (Ca_2MgSi_2O, C_2MS_2). As EMF exists at a high temperature, it could enhance the diffusion and penetration of $Fe^{2+/3+}$ ions to form the $MgFe_2O_4$ phase. At the same time, some $MgAl_2O_4$ spinels exist. However, only $MgAl_2O_4$ phase can be generated without EMF.

1. Introduction

With the development of smelting technology, electromagnetic field (EMF) is widely used in steel metallurgy. For example, EMF is utilized to heat, stir, separate and control flow velocity and shape of molten metal with the uncontact method during the process of long flow rout steelmaking. During the short flow route steelmaking, EMF universally exists in the field of arc/induction furnace and secondary refining [1~3]. So the interfacial reaction of molten slag/refractories for steel metallurgy would be inevitably exposed under EMF. Postchke[4] reported that double layer formed on the interface between liquid slag and refractory materials at a high temperature could be changed by the applied electric potential. Accordingly, the wettability of liquid salg-refractories would be changed, which is described by Lippmann-Young Equation[5~8]. Therefore, the existed EMF can change the potential in double layer and affect slag corrosion of refractories. On the other hand, the corrosion reaction between molten slag and refractories belongs to the electrochemical reaction, which results in electron transfer and exchange[7-8]. The movement of charged particle in EMF can be subject to Lorentz force. So the EMF could affect the kinetic of corrosion reaction between the slag and refractories.

At present, more and more researchers have theoretical knowledge that EMF plays a key role on the reaction of slag/refractories. But a detailed study on this problem has not yet been carried out. For

[1] Author to whom any correspondence should be addressed.

example, how the EMF affects the interfacial reaction? How to prove this influence experimentally? This paper will develop the experiments to research this problem. MgO-C refractories have been chosen in experiments because MgO-C refractories with good thermal shock resistance and excellent slag resistance have been widely used as furnace lining in steelmaking industry and retained an important role in refractories industry[9,10]. The slag resistance experiments of MgO-C refractories were carried out under the condition of EMF and EMF-free. The microstructural change of interfacial layer between slag and MgO-C refractories was investigated by means of x-ray diffractometer(XRD) 、scanning electron microscope(SEM) and EDAX. The influence mechanism of EMF on slag resistance of MgO-C refractories was revealed.

2. Experimental

MgO-C bricks containing 14% carbon and the slag with a basicity(CaO/SiO2) of around 0.8 were used in the experiments. The chemical composition of the slag was shown in Table 1. MgO-C bricks were dried at 200℃ for 24h and cut into the cuboid-shaped samples with the dimension of 20mm×30mm ×100mm. The samples were inserted into the lining of vacuum induction furnace(21WGJL0.025-100-2.5P), where the steel(6Kg) and slag(200g) were then filled. The samples were sintered at 1600℃ ×3h in Ar with the pressure of 0.1MPa. This was the slag resistance experiment in EMF.

The dried MgO-C bricks were cut into the crucible samples with the hole of Φ36×55mm. The outer dimension of crucible samples was 70mm×70mm×70mm. The samples was dried and filled with steel(100g) and slag(50g). Then these samples were embedded in carbon and sintered at 1600 ℃×3 h in a resistance furnace. This was the slag resistance experiment in EMF free.

The phase and microstructure change of slag line for corroded MgO-C bricks was analyzed by means of x-ray diffractometer(XRD), scanning electron microscope(SEM) and EDAX.

Table 1. Chemical composition of slag（mass%）

Fe_2O_3	SiO_2	Al_2O_3	MnO	MgO	CaO	TiO_2	V_2O_5	C/S
22.0	27.5	15.0	3.0	8.0	22.0	2.0	0.5	0.8

3. Results and Discussion

3.1. Effect of EMF on the phase change of corroded MgO-C refractories

Under the condition of EMF and EMF free, the XRD of slag corroded layer for MgO-C refractories illustrates that the spinel and low melting phase are generated (shown in figure 1). The low melting phases in EMF are monticellite ($CaMgSiO_4$, CMS) and forsterite (Mg_2SiO_4, MS). While the low melting phases in EMF free are ehlenite ($Ca_2Al_2SiO_7$, C_2A_2S) and akermanite ($Ca_2MgSi_2O_7$, C_2MS_2).

The SEM of corroded MgO-C refractories in both EMF and EMF free are shown in figure 2. Samples A and B indicate the condition of EMF and EMF free respectively. It is shown in figure 2(A) that sample A has the obvious erosion layer(A1), penetration layer(A2) and original layer(A3). While sample B has the erosion layer (B1) and original layer (B2), the penetration layer is not obvious (shown in figure 2(B)). The particle size of iron deoxidized from Fe_2O_3 is small, while that of penetrated iron is large and occupies the position of the pore. The metal iron in figure 2(A) possesses centralized distribution in the penetration layer, while the metal iron in figure 2(B) distributes near the origin layer.

Lippmann-Young equation[7] is given by:

$$\cos\theta(U) - \cos\theta(0) = \varepsilon_0 \varepsilon_r U^2 / 2d\sigma_{lg} .$$

Where U, θ and ε are the voltage, wetting angle and dielectric constant respectively. σ_{lg} is the interfacial tension between molten slag and refractories. From the equation, EMF could affect the double layer between molten slag and MgO-C refractories, increases the wettabitlity as well as penetration of slag into MgO-C refractories. So there is the penetration layer existed in EMF, while the penetration layer is not discovered in EMF free. EMF enhances the penetration of the slag into MgO-C refractories[11]. Therefore, the reduction reaction between metal oxide in the slag and the carbon in refractories occurs and the formed metal iron distributes in the penetration layer(shown in figure2(A)). In EMF free the reduction reaction occurs in the interfacial layer, where the formed iron metals concentrates(shown in figure2(B)).

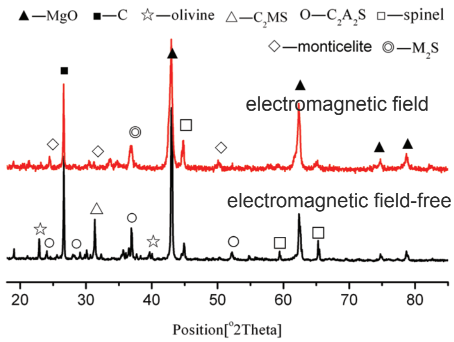

Figure 1 XRD patterns of corroded MgO-C bricks in the slag line under the condition of EMF and EMF free

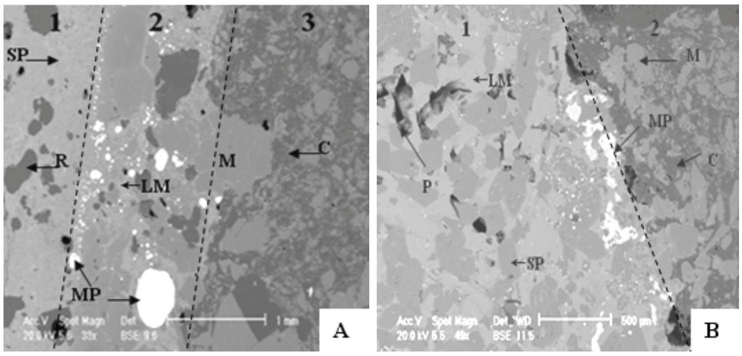

Figure 2 SEM images of the corroded MgO-C bricks in EMF(A) and EMF free(B) LM-low melting phase, M-MgO, MP-metal particle, SP-spinel, R-resin, C-carbon, P-pore)

3.2. Effect of EMF on the Microstructure of the corroded MgO-C refractories

The SEM of corroded layer of MgO-C refractories under the condition of EMF and EMF-free are shown in figure 3 and figure 4 respectively. In EMF, the formed spinel is $MgFe_2O_4$(denoted as point A in figure 3(a) and figure 3(b)). There is a little $MgAl_2O_4$. The particle size of spinels is small and irregular, but they are closed packed. The low melting phase is $CaMgSiO_4$(CMS), denoted as point B in figure 3(a) and figure 3(c). While in EMF free, only $MgAl_2O_4$ spinels distributed in corroded layer are formed(denoted as point A in figure 4). The scaling MgO dissolves into slag and reacts with Al_2O_3 to generate $MgAl_2O_4$ phase. The low melting phases are gehlenite ($Ca_2Al_2SiO_7$, C_2A_2S) and akermanite ($Ca_2MgSi_2O_7$, C_2MS_2), denoted as point B and C in figure 4 respectively.

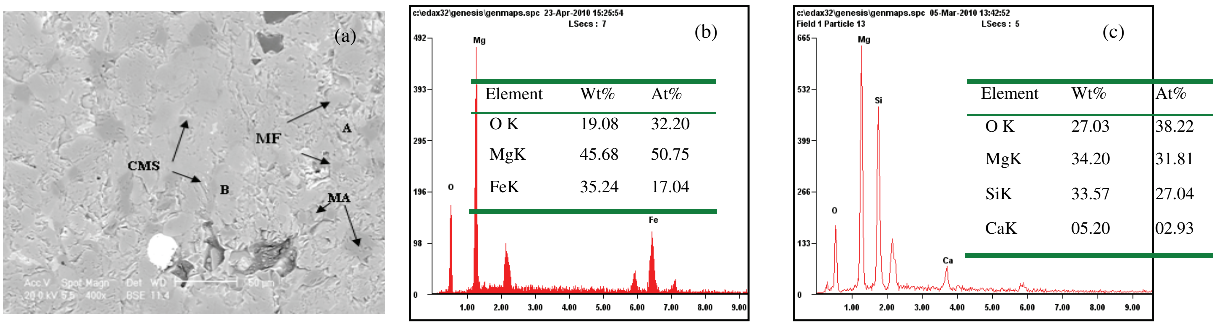

Figure 3 SEM images(a) and EDS patterns(b,c) of the corroded MgO-C bricks in EMF(MF: $MgFe_2O_4$ CMS: $CaMgSiO_4$)

The phase diagram of $MgO\text{-}Fe_2O_3$[12] shows that there is unlimited solid solution and the eutectic temperature is 1713℃. The formulation of solid-state reaction for $MgO\text{-}Fe_2O_3$ is given by: $MgO+Fe_2O_3=MgFe_2O_4$. Thermodynamic calculation[13] shows that the temperature of thermodynamic stability for $MgFe_2O_4$ spinels is about 1200K. During temperature decreasing, the solid solution of MgO and Fe_2O_3 evolves into spinel phases. In EMF, the intensive stirring increases the collision probability between slag and MgO, increases the diffusion of $Fe^{2+/3+}$ and decreases the active energy of $MgFe_2O_4$ generation because of paramagnetic phase of iron oxide at high temperature[14,15]. So $MgFe_2O_4$ spinels exist in EMF, while only $MgAl_2O_4$ spinels exist in EMF free.

EMF increases the wettability of slag to MgO-C refractories and makes MgO dissolve into slag. At the same time, EMF increases the penetration of slag into refractories and decreases the basicity or Ca^{2+} ion concentration of slag in corrosion layer. That leads to the low content of Ca^{2+} in low melting phase. So CMS and MS are the major in the low melt phase, shown in figure 3. While in EMF free, the ability of slag wettability and penetration to MgO-C refractories is weaker. In penetration layer, the Mg^{2+} concentration is low while the Ca^{2+} concentration is high. So the low melting phase in corrosion layer are C_2A_2S and C_2MS_2 as the major phase, shown in figure 4.

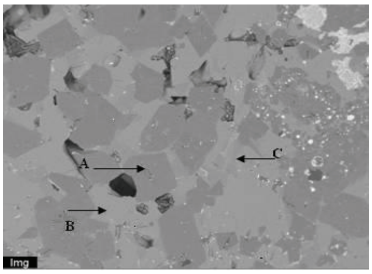

Element	A(wt%)	B（wt%）	C（wt%）
O	34.40	29.44	35.10
Mg	17.92	5.58	
Al	47.69	7.57	11.87
Ca		36.44	25.67
Si		20.98	27.36

Figure 4 SEM images and EDS patterns of the corroded MgO-C bricks in EMF free

4. Conclusions

1) In EMF, there are obvious corrosion and penetration layers in corroded MgO-C refractories. The formed iron concentrates in penetration layer and most of the low melting phase in corrosion layer are monticellite ($CaMgSiO_4$, CMS) and forsterite (Mg_2SiO_4, MS). In EMF free, the formed iron distributes in the interfacial layer between the slag and refractories and most of low melting phase are gehlenite ($Ca_2Al_2SiO_7$, C_2A_2S) and akermanite ($Ca_2MgSi_2O_7$, C_2MS_2).
2) In EMF, scaling of MgO absorbed Fe_2O_3 to form $MgFe_2O_4$ spinels and a little $MgAl_2O_4$ is present. While in EMF free, only $MgAl_2O_4$ existed and distributed in corrosion layer. EMF enhances the corrosion of slag to MgO-C refractories.

5. References

[1] Fujisaki K, Ueyama T, Toh T, Uehara M and Kobayashi S 1998 *IEEE Trans. Magn.* 34(4) 2120
[2] Yu Y and Li B K 2006 *Acta Metallurgica* 42(5) 540
[3] Zhang Q, Jin J Z, Wang T M, Li T Z and Guo J T 2007 *Trans. Nonfer. Metals Soc. China* 17 98
[4] Potschke J 2008 *51st Inter. colloq. Refract.for metall. (*Germany: Eurogress Aachen) P 144
[5] Hopf M I 2008 *51st Inter. colloq. Refract.for metall. (*Germany: Eurogress Aachen) P 225
[6] Aneziris C G and Hampel M 2008 *Int J Appl Ceram Technol.* 5 469
[7] Aneziris C G and Homola F 2004 *Interceram refractories annual* 31 52
[8] Khoroshavin L B and Shcherbatskii B 2005 *Refract. Ind. Ceram.* 05 344
[9] Zhang S, Marriott N J and Lee W E 2001 *J Eur. Ceram.* 2 1037
[10] Li X C, Zhou F and Zhu B Q 2010 *J Chin. Ceram. Soc* 38 1070
[11] Inomoto T, Ogawa Y and Toh T 2003 *ISIJ international* 43 828
[12] Phillips B, Somiya S, and Muan A 1961 *J Am. Ceram. Soc.* 44 167
[13] Liang Y J and Che Y C 1993 *Hand Book for Thermodynamics Data of Inorganic Matter* (Shenyang : East North Industry University Press)
[14] Lioubashevski O, Katz E and Wilner I 2004 *J Phys. Chem. B* 108 5778
[15] Coey J M D and Hinds G 2001 *J. Alloys Comp.* 326 238

Acknowledgments
Authors wish to appreciate the financial support of the National Natural Science Foundation of China (Gant No. 50904048).